IEEE Access
Multidisciplinary | Rapid Review | Open Access Journal

Received May 24, 2019, accepted June 12, 2019, date of publication July 2, 2019, date of current version July 17, 2019.

Digital Object Identifier 10.1109/ACCESS.2019.2926302

Low-Cost Dual-Mechanical-Port Dual-Excitation Machine for Washing Machine Application

NOMAN BALOCH, JUNG-WOO KWON, MUHAMMAD AYUB, AND BYUNG-IL KWON, (Senior Member, IEEE)
Department of Electronic Systems Engineering, Hanyang University, Ansan 15588, South Korea

Corresponding author: Byung-Il Kwon (bikwon@hanyang.ac.kr)

This work was supported in part by the BK21PLUS Program through the National Research Foundation of Korea within the Ministry of Education, and in part by the National Research Foundation of Korea (NRF) grant funded by the Korean Government, Ministry of Science, under Grant NRF-2017R1A2B4007697.

ABSTRACT This paper proposes a low-cost dual-mechanical-port dual-excitation machine for washing machine application. The proposed machine artfully combines two machines (vernier and permanent magnet synchronous machine (PMSM)). An outer vernier rotor is used for the low-speed washing operations, and an inner PMSM rotor is used for the high-speed drying operations of the washing machine. The proposed machine is compared with a similar recently presented machine to verify its cost-effectiveness. Comparison using the finite element analysis (FEA) shows that the ferrite magnets used in the proposed topology are more cost-effective. Furthermore, compared to the existing machine, the power factor of the proposed machine is high during the drying operation; hence, a lower rating inverter is sufficient to drive the machine, which further reduces the overall cost. In addition, the proposed machine provides similar efficiencies as the existing machine for both washing and drying operations.

INDEX TERMS Dual excitation, dual mechanical port, low-cost, PMSM, vernier machine, washing machine.

I. INTRODUCTION

The washing machine is an extensively used domestic appliance and the design of its motor is paramount to ensure its efficiency and cost-effectiveness. There are a few important characteristics a motor designed for a washing machine must possess: 1) wide driving range because it must operate at two speeds (washing and drying), 2) high efficiency at both operation points to minimize energy consumption, 3) low cost of the motor and drive to make the washing machine affordable. A direct drive motor with the abovementioned characteristics will have additional benefits.

Washing machines usually perform two operations: washing and drying. The washing operation is performed at low speeds, such as 50 rpm, and high torque values are required to enable fast start-up at full load; whereas, the drying operation is performed at high speeds, such as 1400 rpm, and requires low torque but high power. The speed required by the drying is typically approximately 28 times as much as that of washing. Different methods are used to achieve the wide operating speed range of the washing machine motor, the commonest of them being the flux-weakening operation [1]–[3]. These operations are usually performed to run the machine at higher speeds. However, flux weakening increases the copper losses of the machine, and poses the risk of demagnetizing the permanent magnets (PMs) [4]. Furthermore, variable flux machines that combine the use of low coercive force (LCF) and constant magnets [5], [6] have been introduced for variable speed applications. The flux of the LCF magnets is weakened using either a negative d-axis current [7], [8] or a separate magnetizing winding [9]. The variable flux machines require complex control to vary the flux density of the LCF magnets. Moreover, there is the risk of permanently demagnetizing the LCF PMs.

The efficiency of the motor for washing machine application has been researched extensively, and many topologies have been proposed [11]–[14]. The efficiency of the washing machine motor is an important design consideration. However, due to the wide operating speed range, the designed machine does not demonstrate equal efficiencies during both operations. The efficiency of the machine is usually high for one operation and very low for the other operation [10].

The associate editor coordinating the review of this manuscript and approving it for publication was Bora Onat.

Furthermore, it is particularly desirable to consumers that a washing machine should be affordable, and the two important factors that impact the overall price of the washing machine are the prices of the motor and the inverter required for running the motor. The cost of the motor depends, to a great extent, on the. Recently, reasonably priced low-cost motors with ferrite magnets have been introduced [15]–[18]. However, the residual flux density (Br) of ferrite magnets is approximately three times lower than that of Neodymium-ferrite-boron (Nd-Fe-B) magnets. In addition, it is necessary to pay special attention to the power factor of the motor for drying operations. Low power factor machines inherently require a higher rating inverter, which increases the overall cost of the washing machine.

Direct drive motors have received extensive attention in recent years because, in addition to other advantages, they improve the reliability of the system by eliminating the backlash and simplifying the mechanical structures [19], [20]. In addition, direct drive motors reduce the noise and vibration of a system. They are incorporated into washing machines to make the machines more compact, according to the needs of user. The washing machine drum is connected directly to the motor shaft, thus eliminating the need for conveyor belts and gearboxes for coupling. Direct drive motors are characterized by high torque density. Therefore, various high torque-density machines, such as vernier machines and dual rotor machines, are the subjects of extensive research. Vernier machines have been recently acknowledged as a promising candidate for direct drive applications due to their high torque density [21], [22]. However, because of their high core losses and low power factor, they cannot be used for the drying operation of the machine.

Dual-rotor machines have been introduced in the literature [23]–[25]. These machines feature two rotors connected to a single shaft, which, compared to a single rotor topology, achieves a higher torque density. In [25], a dual-rotor hybrid permanent magnet machine is proposed for the traction application in which the outer rotor is a surface permanent magnet (SPM) rotor, and the inner rotor is a synchronous reluctance rotor. However, the two rotors are connected to a single shaft. Furthermore, dual mechanical port machines, with dual decoupled rotors, have been attracting scholarly attention [26], [27]. However, they have a single stator with two windings, which raises mutual coupling issues between two sets of windings [23]. Recently, a dual output stator-PM machine has been introduced to achieve high efficiency at the two operating points of a washing machine [28]. For comparison, the recently introduced machine will subsequently be referred to as the existing machine. Although the existing machine provides high efficiency for both washing and drying operations, it has a few shortcomings. Firstly, it deploys high-cost NdFeB magnets that increase the cost of the machine considerably. Secondly, the existing machine uses a flux-reversal machine for the drying operation. The flux-reversal machine is a type of flux-modulation machine. Hence, its operating frequency is high, and its core losses

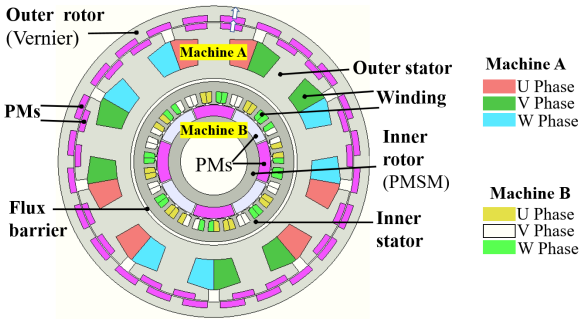

FIGURE 1. Configuration of proposed topology.

are correspondingly high. Thirdly, its power factor is low during drying operation. Therefore, A high rating inverter is required, which increases the overall cost of the system.

In this paper, a low-cost dual-mechanical-port dual-excitation machine is proposed for the washing machine application to circumvent the abovementioned demerits of the existing machine. The proposed motor is more cost-effective because of the cheaper PM and inverter. This is due to the alternate topologies proposed for the outer and inner rotors. Moreover, the proposed machine provides similar efficiencies as the existing machine. The proposed topology and its working principle are explained in Section II. The design considerations of the proposed topology are elaborated on in Section III. The performance analysis of the proposed machine using the finite element method is presented in Section IV. Finally, to verify the merits of the proposed machine, it is compared with the existing machine in terms of efficiency, power factor, and magnet price.

II. TOPOLOGY AND WORKING PRINCIPLE

A. TOPOLOGY

The configuration of the proposed topology is shown in Fig. 1. It is a combination of two machines, one nested into the other. The outer rotor and outer stator are referred to as Machine A, whereas the inner stator and inner rotor are referred to as Machine B.

Machine A is a dual-consequent-pole vernier machine [29]. It has an outer-rotor and inner-stator topology. It deploys one set of low-cost PMs (ferrite) on the rotor and another set of the PMs of the same grade on the stator. The stator of Machine A is comprised of the flux-modulation teeth with three-phase armature windings. Moreover, PMs are inserted between the flux-modulation teeth that are radially magnetized. The rotor of Machine A is composed of consequent-pole PMs along with iron teeth. The flux of the stator PMs and rotor PMs are both channeled outwards. It should be noted that the dual-consequent-pole vernier machine is selected for washing operation because of its high torque density. This is necessary because low-cost ferrite magnets with low Br are desirable for their cost-effectiveness, which otherwise will reduce the torque density of the machine, which in turn will affect the efficiency of the machine. Hence, the dual-consequent-pole vernier machine

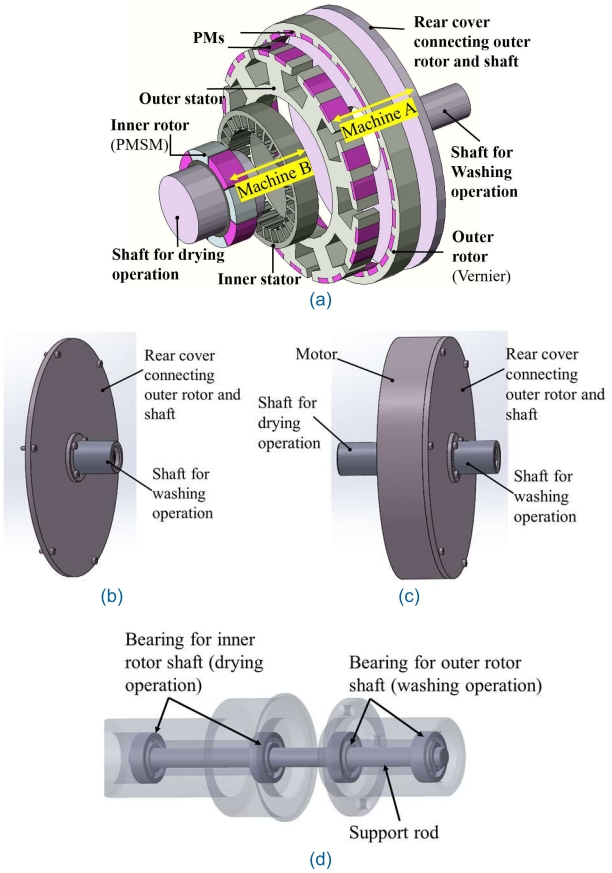

FIGURE 2. Exploded view of proposed topology (a) Exploded view (b) outer rotor and shaft connection method (c) motor with two shafts (d) bearings for shafts.

is desirable because its use of ferrite magnets ensures affordability and high efficiency for low-speed operations.

Machine B is a conventional surface-type PMSM. The stator is composed of 27 slots with four pole-pairs of armature windings, whereas the rotor consists of four pole-pairs of ferrite magnets. The number of slots and poles are selected to achieve the lowest possible torque ripple. A flux barrier is incorporated between the stators of Machines A and B (Fig. 1), which eliminates the magnetic coupling between the two machines. It is worth noting that the drying operation requires low torque. Therefore, a PMSM with ferrite magnets is the optimal choice for it because of its low-cost and high efficiency for high-speed operations.

The exploded view of the proposed topology is shown in Fig. 2(a). To perform washing and drying operations, two shafts are introduced to both sides of the machine. The inner rotor is directly connected to one side of the shaft, and it is used for the drying operation. The outer rotor is connected to a rear cover that is attached to the shaft on the other side, as shown in Fig. 2(b). It is connected such that when the outer rotor rotates, the connected cover rotates, which causes the shaft on the other side to rotate, thus enabling washing operations.

It should be noted that the washing drum and drying drum are not connected to each other. The outer rotor is connected to the washing drum, and the inner rotor is connected to the drying drum. The two shafts are independent of each other, as shown in Fig. 2(c). When the outer rotor shaft rotates, the inner rotor may or may not rotate, depending on the requirement of the end user during the drying operation. To keep the two shafts independent of each other, bearing was installed on both sides of each shaft as shown in Fig. 2(d). Due to these bearings, both shafts can rotate independently of each other.

B. WORKING PRINCIPLE

Machine A is a dual-consequent-pole vernier machine. It is the combination of a stator consequent-pole PM vernier machine and a rotor consequent-pole PM vernier machine. Its working principle is based on the flux modulation principle [30], [31]. Machine A satisfies equation (1) to generate the flux modulation effect:

$$Z_r = Z_s - P \tag{1}$$

where Z_r is the number of rotor pole pairs, Z_s is the number of stator slots, and P is the number of armature pole pairs.

The flux from the rotor PMs is modulated by the stator flux-modulation teeth that produce a component equal to the stator-winding pole-pairs in the airgap flux density. The flux from the stator PMs is modulated by the rotor iron teeth, and produces a component equal to the winding pole pairs in the airgap. Therefore, the flux of both the rotor and stator PMs are modulated, and induce a back electromagnetic force (EMF) of the same frequency in the stator windings of Machine A. The working principle can be better explained by analyzing the airgap flux density in three conditions: with only rotor PMs, with only stator PMs, and with both stator and rotor PMs. The outer airgap flux-density of Machine A in these three conditions is shown in Fig. 3(a), 3(b), and 3(c), respectively.

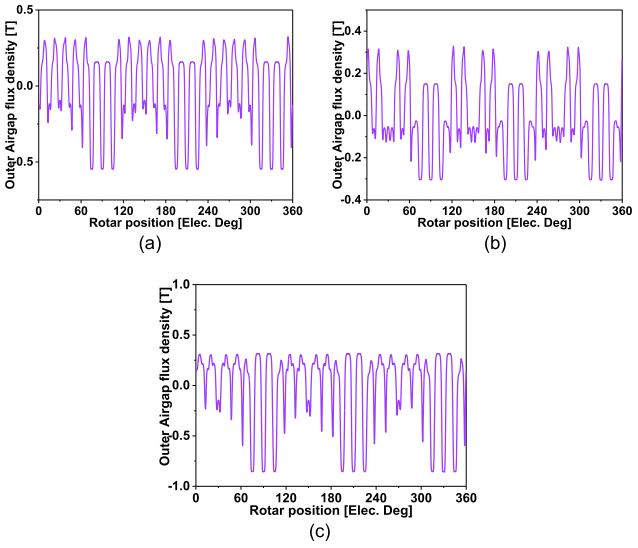

FIGURE 3. Airgap flux density (a) only rotor PMs (b) only stator PMs (c) both stator and rotor PMs.

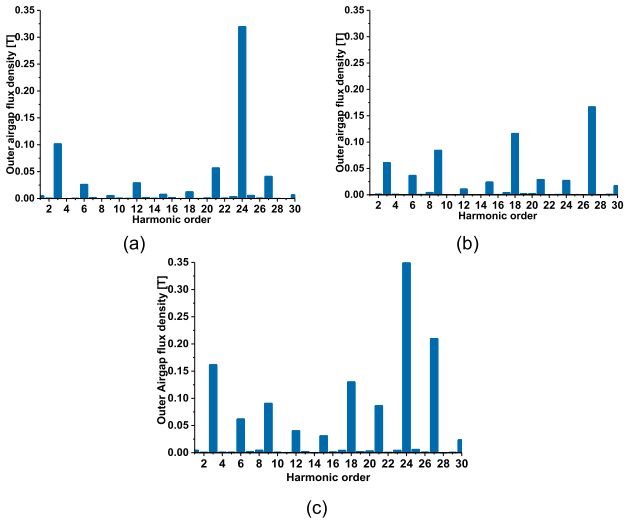

FIGURE 4. Airgap flux density harmonic spectra (a) only rotor PMs (b) only stator PMs (c) both stator and rotor PMs.

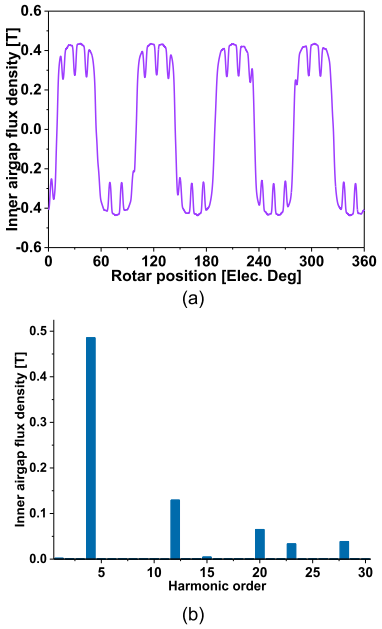

FIGURE 5. Airgap flux density Machine B (a) Waveform (b) Harmonic spectra.

The measurement of the airgap flux density reveals 24 pole pairs, because there are 24 pole pairs of rotor under all the three conditions. The harmonic spectra of the outer airgap flux density in the three conditions are shown in Fig. 4(a), 4(b), and 4(c), respectively. In Fig. 4(a), the harmonics of the airgap flux density with only rotor PMs are shown. The two working harmonics are the 3rd pole-pair-modulated component and the 24th pole-pair component, indicating the number of rotor PMs. The values of the 3rd and 24th harmonics are approximately 0.1 T and 0.33 T, respectively. The 3rd harmonic is the modulated component that is obtained under two conditions (with only stator PMs and only rotor PMs). When both stator and rotor PMs are used, as shown in Fig. 4(c), the magnitude of this component is summed, which increases the back EMF, and consequently, the torque density in this topology. Moreover, additional working harmonics (such as 6, 12, 15, 21, and 30) are introduced in the airgap that produces the torque. This is because they are tooth harmonics of the 3rd harmonic (fundamental harmonic). The proposed Machine A has nine stator slots; thus, the 9k plus or minus 3 are tooth harmonics. Furthermore, some harmonics (such as 18 and 27) that result from the stator PM magneto-motive force (MMF) (18-pole pair) and air-gap permeance harmonic (9-pole pair), produce torque ripple. The 18th harmonic results from the stator PM MMF (18-pole pair) and the dc-term of the air-gap permeance; thus, it is stationary, and will not produce fundamental back EMF and average torque. The 27th harmonic is produced by the stator PM MMF (18-pole pair) and 9-pole-pair stator permeance; thus, it is also stationary and will not produce fundamental back-EMF. Machine A is utilized at the low speed of 50 rpm because of its higher torque density. It should be noted that the ferrite PMs are used to reduce the cost of the machine.

Machine B functions like a synchronous machine, because it is a conventional PMSM. The rotor PMs and stator windings have equal numbers of pole pairs. The airgap flux density and harmonic spectra of Machine B (inner airgap) are shown in Fig. 5(a) and 5(b), respectively. It can be observed that the airgap shows the 4-pole-pair main component, the number of the rotor pole pairs. The equal pole pairs of the stator and rotor interact to produce torque. Moreover, because Machine B is a conventional PMSM with few pole pairs, its armature frequency is not high, thus limiting the core losses of the machine. Machine B is used for the drying operation (1400 rpm). However, additional harmonics, such as the 12th and 20th, are present in the airgap flux density, thus producing torque ripple.

III. DESIGN CONSIDERATIONS FOR THE PROPOSED TOPOLOGY

The design flow chart of the proposed topology is shown in Fig. 6. Initially, the topology of Machine A is selected. As we intend to use ferrite magnets at the low speed of 50 rpm, a machine with high torque density is required to compensate for the low residual flux-density of the ferrite magnets. Thus, for Machine A, the double-consequent-pole vernier machine was selected because of its higher torque density that was achieved based on the double flux modulation principle discussed earlier. To maintain the compactness of the washing machine, the outer diameter of the motor should not be very large, neither should the stack be very long Therefore, the outer diameter of the machine was set to 280 mm, while the stack length was set to 25 mm. Moreover, natural cooling is selected for the machine.

Initially, an outer-rotor vernier machine is designed for the washing operation. Because high efficiency is required at 50 rpm, it is necessary to minimize the losses of the machine. At 50 rpm, the major losses of the machine are copper losses.

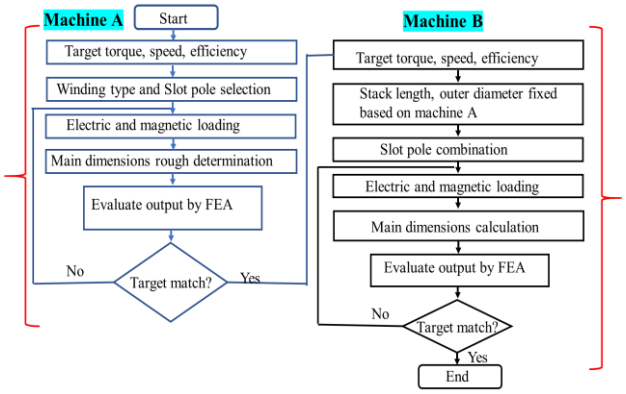

FIGURE 6. Design flow chart of Proposed topology.

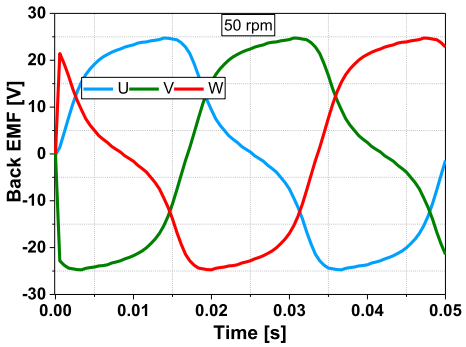

FIGURE 7. Back EMF of Machine A.

Hence, to minimize the copper losses, concentrated winding is employed in the stator of Machine A. The concentrated winding has a short end winding length, which corresponds to minimal copper losses. In addition, the pole ratio is also taken into consideration when selecting the pole-slot combination. The pole ratio is the ratio of the rotor pole pairs to the stator pole pairs; it affects the torque capability of the vernier machine. The pole-slot combination of Machine A is selected such that the pole ratio is 8. This pole ratio produces a high torque density with the employed fractional-slot concentrated winding. The initial main parameters, such as the airgap diameter, number of turns/phase, and stator current of the machine, are determined based on the design algorithm. Subsequently, finite element analysis (FEA) was performed to refine the parameters. Additional design considerations were made to select the optimal split ratio, which is defined as the ratio of the rotor's inner diameter to the outer diameter. The higher split ratio provides a higher torque density; however, the resultant reduction in the width of the rotor core causes saturation that inevitably results in higher torque ripple and higher core losses. Following the FEA, the split ratio of 0.9 was determined to be the ideal. Furthermore, geometrical parameters, such as the auxiliary tooth width, slot depth, and slot opening, have a significant impact on the torque performance in vernier machines. These parameters were optimized using the genetic algorithm. All the results presented for Machine A are the final optimized results.

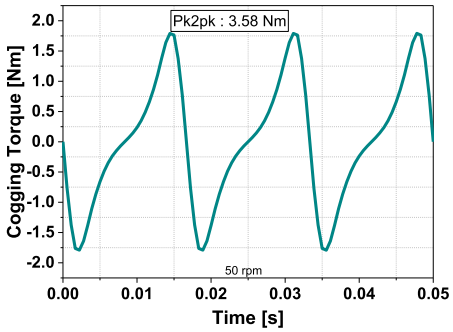

FIGURE 8. Cogging torque of Machine A.

After finalizing the parameters of Machine A, the thickness of the flux barrier was determined using iterative optimization to eliminate the magnetic coupling between Machines A and B. Because Machine B is to be nested inside the available space within Machine A, the outer diameter of Machine B cannot exceed the inner diameter of the flux barrier. Furthermore, the overall size of the machine remains unchanged because the stack length of Machine B is set to 25 mm, same as that of Machine A. The machine design algorithm is adhered to, and the main dimensions of Machine B are determined and refined using FEA. It should be noted that it was discovered that the slot area for coils was small in Machine B because of size restrictions. Hence, the coil diameter size was finally designed to be small to adjust the required number of turns, resulting in high copper losses in Machine B. Additionally, semi-closed slots were selected for Machine B to minimize the cogging torque. The width and height of the inner-rotor PMs were finalized based on iterative optimization. The main parameters of the proposed machine are shown in Table 1.

IV. PERFORMANCE ANALYSIS AND COMPARISON

In this section, the performance of the proposed machine is analyzed using 2D FEA. The commercial software, "JMAG version 17," was used for the FEA.

A. PERFORMANCE OF MACHINE A

The back EMF of Machine A during the washing operation (50 rpm) is shown in Fig. 7. Distortions can be seen in the back EMF. This is because of the harmonics in the outer airgap flux density of Machine A due to the dual-consequent-pole structure of the machine.

The cogging torque of Machine A during the washing operation is shown in Fig. 8. It can be observed that a peak-to-peak cogging torque of 3.58 Nm is obtained in the proposed Machine A. This is attributable to the selected pole-slot combination for Machine A. The selected pole-slot combination and the dual-consequent-pole structure produce higher torque density; however, its drawback is the higher cogging torque.

The output torque of Machine A is shown in Fig. 9. An average torque of 17.4 Nm is obtained with a torque ripple of 15%. The torque ripple is mainly attributable to the additional harmonics in the airgap flux density. The flux

TABLE 1. Main parameters of conventional, existing, and proposed topology.

Parameters	Unit	Value				
Machine type	-	Conventional	Existing		Proposed	
Sub-category	-	-	Machine I	Machine II	Machine A	Machine B
Machine outer diameter	mm	280				
Stack length	mm	25				
Flux barrier length	mm	-	3			
Airgap length	mm	1	1	0.5	1	0.5
Stator outer diameter	mm	265	239	164	250	148
Stator inner diameter	mm	200	170	108.8	154	106
No. of turns / phase	-	396	400	900	480	540
No. of slots	-	36	12	6	9	27
PM pole pairs	-	24	24	6	24	4
PM volume	mm^3	48000	22200	25475	124000	81625
PM grade	-	NdFeB (Neomax-50)			Ferrite (YBM_9BE)	
PM residual flux density	-	1.44			0.4	

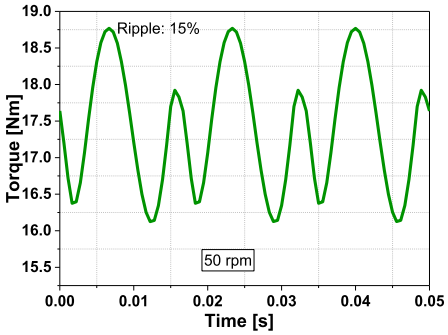

FIGURE 9. Output torque of Machine A.

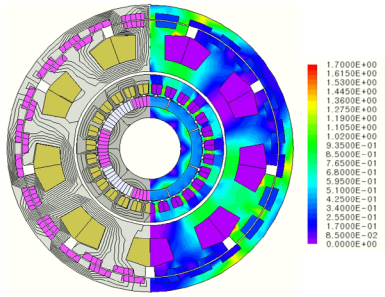

FIGURE 10. Flux lines and flux density distribution.

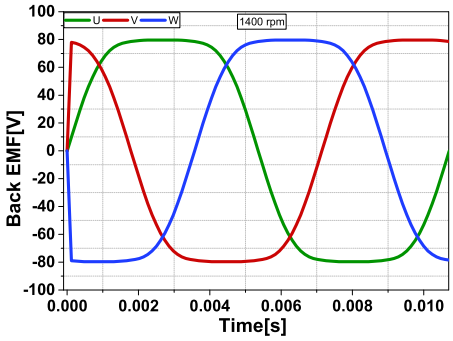

FIGURE 11. Back EMF of machine B.

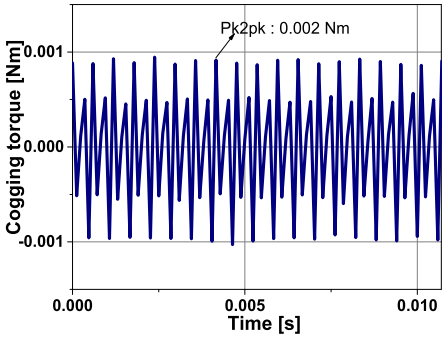

FIGURE 12. Cogging torque of machine B.

lines and flux density of the proposed machine at 50 rpm is shown in Fig. 10. It can be observed that there is no coupling between Machines A and B. Moreover, most components of the machine operate under the saturation limit of 1.8 T.

The copper and iron losses of the proposed machine were calculated to obtain the efficiency calculations. The efficiency of Machine A was calculated using equation (2):

$$\eta = \frac{P_{out}}{P_{out} + P_{cu} + P_{iron}} \times 100 \tag{2}$$

where P_{out}, P_{cu}, and P_{iron} represent the output power, copper losses, and iron losses, respectively. The iron losses of the proposed machine were found to be 2.5 W. The copper losses were higher. The efficiency of the proposed Machine A based on the copper and iron losses was 89.4%.

B. PERFORMANCE OF MACHINE B

Machine B is used for the drying operations of the washing machine. The drying operation is performed at a high speed of 1400 rpm.

The back EMF of Machine B at 1400 rpm is shown in Fig. 11. It can be observed that smooth and sinusoidal back EMF is received. The cogging torque of Machine B is shown in Fig. 12. It can be observed that the peak-to-peak

TABLE 2. Performance comparison of conventional, existing, and proposed topology.

Parameters	Unit	Value					
Machine type	-	Conventional		Existing		Proposed	
Operating mode	-	Washing	Drying	Washing	Drying	Washing	Drying
Speed	rpm	50	1400	50	1400	50	1400
Back EMF	V	9.7	216.6	10.3	190.1	18	66
Terminal voltage	V	23.3	311	23.3	311	28	73.7
Armature current	A	4.9	2	4.15	1.5	1.7	2.95
Average torque	Nm	17	4.1	17	4.1	17.1	4.1
Torque ripple	%	15.6	29.7	7.3	5.5	15	3.8
Power factor	-	0.98	0.98	0.86	0.74	0.78	0.98
Iron loss	W	3	131	3.5	30.7	2.47	5
Copper loss	W	18.4	3	7.7	24.3	8.1	60
Power	W	89.5	601.1	89.5	601.1	89.5	601.1
Efficiency	%	80.6	82	88.8	91.6	89.4	90.2
Magnet cost	$USD	6.34*		6.28*		4.5**	
	*NdFeB = 17.6 $/ kg			** Ferrite = 4.5 $/kg			

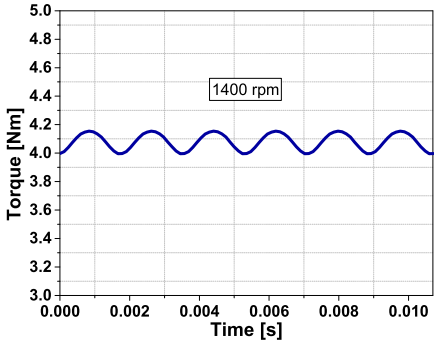

FIGURE 13. Output torque of machine B.

cogging torque obtained is 0.002 Nm. This value is very low, and is caused by the selected pole-slot combination. The torque required for the drying operation is usually low. The obtained torque of Machine B is shown in Fig. 13. An average torque of 4.1 Nm is obtained, with a torque ripple of 3.8%. However, this has minimal effect on the overall torque ripple because the cogging torque of the machine is very low. The additional harmonics in the airgap flux density (Fig. 5) also contribute to the torque ripple in the inner rotor.

The copper and iron losses of the machine were found to be 60 W and 5 W, respectively. The high copper losses of the machine are due to the small slot area that causes a smaller coil diameter in the machine, leading to increased coil resistance. Moreover, Machine B also utilized low-cost ferrite magnets; therefore, the magnetic loading of the machine was low. Hence, a higher electric load was used. The iron losses of the machine were found to be low because of the lower magnetic loading and lower frequency in Machine B. The efficiency of Machine B for the drying operation was found to be 90.2%.

C. PERFORMANCE COMPARISON OF EXISTING AND PROPOSED TOPOLOGIES

To verify the effectiveness of the proposed topology, it is compared with the conventional topology used in washing machines [32] as well as with the existing machine [28]. For a fair comparison, the outer diameter, stack length, rated speed, airgap length, flux-barrier length, and output power of both machines are the same. The main parameters of the conventional machine, existing machine, and the proposed machines are listed in Table 1. It should be noted that the PM volume of the proposed machine is much higher than those of the conventional and existing machine, because ferrite PMs having density of 5 g/cm^3 with a residual flux density of 0.4 T are utilized in the proposed machine, and NdFeB magnets having density 7.5g/cm^3 with a residual flux density of 1.44 T are utilized in the conventional and existing machine.

The comparison of the performances of all the topologies is presented in Table 2. At 50 rpm, the proposed machine exhibits a higher back EMF, compared to the conventional and existing machine. The torques of the three machines are the same, because they are compared at the same power. The power factor of the proposed machine is slightly lower, compared to the existing machine because of its lower magnetic loading. In addition, although the proposed machine provides better efficiency at 50 rpm, its ripple is high, compared to the existing machine.

At 1400 rpm, the torque ripple of the proposed machine is lower, compared to the existing machine. Additionally, the power factor of the proposed machine is 0.98, much higher, compared to that of existing machine, 0.74. Therefore, the terminal voltages of the proposed machine are much lower than that of the existing machine. Hence, a lower rating inverter is required to drive the machine, which will decrease the cost of the machine. Although the proposed machine employs a

higher magnet volume, the cost price of ferrite PMs per kg is much lower than that of NdFeB magnets. Therefore, overall, the PMs used in the proposed machine are cheaper. The proposed machine provides a similar efficiency as the existing machine at both speeds, even with the usage of low-cost ferrite magnets. This is owing to the better performance of the selected topologies for Machine A (washing operation) and B (drying operation). The power factor of the conventional machine is the same as the proposed drying operation; however, its efficiency is lower. The overall cost of the machine will be further low because of the high power factor of the proposed topology during drying operation.

V. CONCLUSIONS

This paper proposed a topology to achieve high efficiency at the two operations points of a washing machine while ensuring low overall cost compared to an existing machine. The proposed topology was an integration of two machines, a dual-consequent-pole vernier machine and a permanent magnet synchronous machine (PMSM). The design considerations of the proposed machine were presented in detail in this paper. In addition, the proposed machine was compared with an existing dual-output machine to demonstrate the superiority of the proposed machine. The results showed that the proposed machine provided high efficiencies for both the washing and drying operations. The power factor for the drying operation of the proposed machine was high. Therefore, the inverter rating was reduced. Moreover, the PMs were also cheaper, because low-cost ferrite magnets were utilized. Therefore, the drive will be more affordable than the existing machine.

REFERENCES

[1] O. Payza, Y. Demir, and M. Aydin, "Investigation of losses for a concentrated winding high-speed permanent magnet-assisted synchronous reluctance motor for washing machine application," *IEEE Trans. Magn.*, vol. 54, no. 11, Nov. 2018, Art. no. 8207606.

[2] S. Ni and U. Schaefer, "Optimization of a spoke-type permanent magnet motor by combination of genetic algorithm and finite element method," in *Proc. 13th Int. Conf. Elect. Mach. (ICEM)*, Sep. 2018, pp. 892–898.

[3] A. Dianov and S.-T. Lee, "Novel IPMSM drive for compact washing machine," in *Proc. 31st Int. Telecommun. Energy Conf. (INTELEC)*, Oct. 2009, pp. 1–7.

[4] J. A. Tapia, F. Leonardi, and T. A. Lipo, "Consequent-pole permanent-magnet machine with extended field-weakening capability," *IEEE Trans. Ind. Appl.*, vol. 39, no. 6, pp. 1704–1709, Nov./Dec. 2003.

[5] S. Maekawa, K. Yuki, M. Matsushita, I. Nitta, Y. Hasegawa, T. Shiga, T. Hosoito, K. Nagai, and H. Kubota, "Study of the magnetization method suitable for fractional-slot concentrated-winding variable magnetomotive-force memory motor," *IEEE Trans. Power Electron.*, vol. 29, no. 9, pp. 4877–4887, Sep. 2014.

[6] J. Chen, J. Li, and R. Qu, "Analysis, modeling, and current trajectory control of magnetization state manipulation in variable-flux permanent magnet machines," *IEEE Trans. Ind. Electron.*, vol. 66, no. 7, pp. 5133–5143, Jul. 2019.

[7] N. Limsuwan, T. Kato, K. Akatsu, and R. D. Lorenz, "Design and evaluation of a variable-flux flux-intensifying interior permanent-magnet machine," *IEEE Trans. Ind. Appl.*, vol. 50, no. 2, pp. 1015–1024, Mar./Apr. 2014.

[8] J.-M. Kim, J.-Y. Choi, K.-S. Lee, S.-H. Lee, "Design and analysis of surface-mounted-type variable flux permanent magnet motor for wide-speed range applications," *IEEE Trans. Magn.*, vol. 51, no. 11, Nov. 2015, Art. no. 8111004.

[9] H. Yang, S. Lyu, H. Lin, Z. Q. Zhu, F. Peng, E. Zhuang, S. Fang, and Y. Huang, "Stepwise magnetization control strategy for dc-magnetized memory machine," *IEEE Trans. Ind. Electron.*, vol. 66, no. 6, pp. 4273–4285, Jun. 2019.

[10] C.-S. Jin, D.-S. Jung, K.-C. Kim, Y.-D. Chun, H.-W. Lee, and J. Lee, "A Study on Improvement Magnetic Torque Characteristics of IPMSM for Direct Drive Washing Machine," *IEEE Trans. Magn.*, vol. 45, no. 6, pp. 2811–2814, Jun. 2009.

[11] J. S. Yoo, H. Jang, S. Cho, G. S. Lee, S.-J. Ko, S. Bae, H.-J. Lee, H. Liu, J. Lee, and H. So, "Design of rotor with novel barrier for power improvement of spoke-type permanent magnet synchronous motor," in *Proc. 21st Int. Conf. Elect. Mach. Syst. (ICEMS)*, Oct. 2018, pp. 252–255.

[12] S. M. Castano, R. Yang, C. Mak, B. Bilgin, and A. Emadi, "External-rotor switched reluctance motor for direct-drive home appliances," in *Proc. 44th Annu. Conf. IEEE Ind. Electron. Soc. (IECON)*, Oct. 2018, pp. 514–521.

[13] M. Asgar, E. Afjei, A. Behbahani, and A. Siadatan, "A 12/8 double-stator switched reluctance motor for washing machine application," in *Proc. 6th Power Electron., Drive Syst. Technol. Conf. (PEDSTC)*, Feb. 2015, pp. 168–172.

[14] A. Tap, L. Xheladini, T. Asan, M. Imeryuz, M. Yilmaz, and L. T. Ergene, "Effects of the rotor design parameters on the torque production of a PMaSynRM for washing machine applications," in *Proc. Int. Conf. Optim. Elect. Electron. Equip. (OPTIM) & Intl Aegean Conf. Elect. Mach. Power Electron. (ACEMP)*, May 2017, pp. 370–375.

[15] Y. Kong, M. Lin, M. Yin, and L. Hao, "Rotor structure on reducing demagnetization of magnet and torque ripple in a PMa-synRM with ferrite permanent magnet," *IEEE Trans. Magn.*, vol. 54, no. 11, Nov. 2018, Art. no. 8108705.

[16] Y. Chen, Y. Ding, X. Li, and X. Zhu, "Design and analysis of less-rare-Earth double-stator modulated machine considering multioperation conditions," *IEEE Trans. Appl. Supercond.*, vol. 28, no. 3, Apr. 2018, Art. no. 5201405.

[17] Z. S. Du and T. A. Lipo, "Torque performance comparison between a ferrite magnet Vernier motor and an industrial interior permanent magnet machine," *IEEE Trans. Ind. Appl.*, vol. 53, no. 3, pp. 2088–2097, May/Jun. 2017.

[18] A. Tap, L. Xheladini, M. Yilmaz, M. Imeryuz, T. Asan, and L. T. Ergene, "Comprehensive design and analysis of a PMaSynRM for washing machine applications," *IET Electr. Power Appl.*, vol. 12, no. 9, pp. 1311–1319, Nov. 2018.

[19] J. Yu and C. Liu, "Design of a double-stator magnetless vernier machine for direct-drive robotics," *IEEE Trans. Magn.*, vol. 54, no. 11, Nov. 2018, Art. no. 8105805.

[20] Y. Cheng, D. Li, W. Kong, R. Qu, and F. Lin, "Electromagnetic design of a large-scale double-stator direct driving HTS wind generator," *IEEE Trans. Appl. Supercond.*, vol. 28, no. 4, Jun. 2018, Art. no. 5205105.

[21] F. Zhao, T. A. Lipo, B.-I. Kwon, "A novel dual-stator axial-flux spoke-type permanent magnet Vernier machine for direct-drive applications," *IEEE Trans. Magn.*, vol. 50, no. 11, Nov. 2014, Art. no. 8104304.

[22] Y. Gao, R. Qu, D. Li, and F. Chen, "Force ripple minimization of a linear Vernier permanent magnet machine for direct-drive servo applications," *IEEE Trans. Magn.*, vol. 53, no. 6, Jun. 2017, Art. no. 7001905.

[23] X. Ren, D. Li, R. Qu, W. Kong, X. Han, and T. Pei, "Analysis of spoke-type brushless dual-electrical-port dual-mechanical-port machine with decoupled windings," *IEEE Trans. Ind. Electron.*, vol. 66, no. 8, pp. 6128–6140, Aug. 2019.

[24] R. Qu and T. A. Lipo, "Dual-rotor, radial-flux, toroidally wound, permanent-magnet machines," *IEEE Trans. Ind. Appl.*, vol. 39, no. 6, pp. 1665–1673, Nov./Dec. 2003.

[25] Y. Li, D. Bobba, and B. Sarlioglu, "Design and optimization of a novel dual-rotor hybrid PM machine for traction application," *IEEE Trans. Ind. Electron.*, vol. 65, no. 2, pp. 1762–1771, Feb. 2018.

[26] X. Ren, D. Li, R. Qu, and T. Zou, "A brushless dual-mechanical-port dual-electrical-port machine with spoke array magnets in flux modulator," *IEEE Trans. Magn.*, vol. 53, no. 11, Nov. 2017, Art. no. 8110706.

[27] X. Sun, M. Cheng, W. Hua, and L. Xu, "Optimal design of double-layer permanent magnet dual mechanical port machine for wind power application," *IEEE Trans. Magn.*, vol. 45, no. 10, pp. 4613–4616, Oct. 2009.

[28] J.-W. Kwon and B.-I. Kwon, "High-efficiency dual output stator-PM machine for the two-mode operation of washing machines," *IEEE Trans. Energy Convers.*, vol. 33, no. 4, pp. 2050–2059, Dec. 2018.

[29] W. Zhao, X. Sun, J. Ji, and G. Liu, "Design and analysis of new Vernier permanent-magnet machine with improved torque capability," *IEEE Trans. Appl. Supercond.*, vol. 26, no. 4, Jun. 2016, Art. no. 5201505.
[30] N. Baloch, B.-I. Kwon, and Y. Gao, "Low-cost high-torque-density dual-stator consequent-pole permanent magnet Vernier machine," *IEEE Trans. Magn.*, vol. 99, no. 11, Nov. 2018, Art. no. 8206105.
[31] Z. Liang, Y. Gao, D. Li, and R. Qu, "Design of a novel dual flux modulation machine with consequent-pole spoke-array permanent magnets in both stator and rotor," *CES Trans. Elect. Mach. Syst.*, vol. 2, no. 1, pp. 73–81, Mar. 2018.
[32] J.-M. Kim, J.-Y. Choi, S.-H. Lee, and S.-M. Jang, "Characteristic analysis and experiment of surface-mounted type variable-flux machines considering magnetization/demagnetization based on electromagnetic transfer relations," *IEEE Trans. Magn.*, vol. 50, no. 11, Nov. 2014, Art. no. 8600804.

NOMAN BALOCH was born in 1987. He received the B.S. degree in electronics engineering from the Balochistan University of Information Technology, Engineering and Management Sciences (BUITEMS), Quetta, Pakistan, in 2010. He is currently pursuing the M.S. and PhD. degrees from the Department of Electronics System Engineering, Hanyang University, Ansan, South Korea.

From 2010 to 2015, he was the Deputy Assistant Director of the National Database and Registration Authority (NADRA), Pakistan. His research interest includes the design and control of electrical machines.

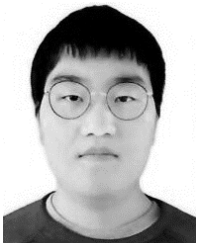

JUNG-WOO KWON was born in 1992. He received the B.S. degrees in bio-nano engineering and electrical engineering from Hanyang University, Ansan, South Korea, in 2015, where he is currently pursuing the M.S. and Ph.D. degrees with the Department of Electronics System Engineering. His research interest includes electric machines, especially on motors.

MUHAMMAD AYUB was born in Quetta, Pakistan. He received the B.S. degree from the Balochistan University of Information Technology, Engineering and Management Sciences (BUITEMS), Quetta, Pakistan, in 2008. He is currently pursuing the Ph.D. degree with the Department of Electrical and Electronic Engineering, Hanyang University, Ansan, South Korea. He was a Lecturer with BUITEMS. His research interest includes electric machine design and control.

BYUNG-IL KWON was born in 1956. He received the B.S. and M.S. degrees in electrical engineering from Hanyang University, Ansan, South Korea, in 1981 and 1983, respectively, and the Ph.D. degree in electrical engineering, machine analysis from The University of Tokyo, Tokyo, Japan, in 1989. From 1989 to 2000, he was a Visiting Researcher with the Faculty of Science and Engineering Laboratory, University of Waseda, Tokyo, Japan. In 1990, he was a Researcher with the Toshiba System Laboratory, Yokohama, Japan. In 1991, he was a Senior Researcher with the Institute of Machinery and Materials Magnetic Train Business, Daejeon, South Korea. From 2001 to 2008, he was a Visiting Professor with the University of Wisconsin–Madison, Madison, WI, USA. He is currently a Professor with Hanyang University. His research interest includes the design and control of electric machines.